

The influence of disc friction losses and labyrinth losses on efficiency of high head Francis turbine

D Čelič¹ and H Ondráčka²

¹Independent Researcher, Damjan Čelič, s.p., Novo mesto, Slovenia

²Hydraulic Designer, Scandic Energy, Rakkestad, Norway

E-mail: damjan.celic@gmail.com

Abstract. CFD is a very powerful tool, which significantly reduces the need for model testing of Francis turbines. Numerical models are constructed so as to cover all the essential geometric and physical properties of the physical models. However, for the sake of simplicity, some geometric details are often neglected. In case of Francis turbines, labyrinths are usually not included in the numerical model and consequently the disc friction losses and labyrinth losses are ignored. This may lead to inaccurate prediction of turbine efficiency. In our study we have investigated the importance of considering all the geometrical details of labyrinth for the accurate prediction of efficiency of high head Francis turbine. The research was performed by using commercial software Numeca FINETM/Turbo.

1. Introduction

Labyrinth seals are the most common type of non-contact seal between the runner and the turbine covers, which is widely used in turbo-machinery. Water leaking through a labyrinth will cause reduced efficiency since it will not be utilized by the runner. The leakage flow through the seals depends upon the size of the gap [1]. For a new turbine the labyrinth gap will be small and the leakage will be low. As the seals wear, the gap increases and so does the leakage. The labyrinth consists of two parts, a static seal connected to the covers and a rotating part connected to the runner.

In the past, much effort has been put into determination of volumetric and mechanical efficiencies and leakage behavior of Francis turbine [2]. Mechanical and volumetric efficiencies have been expressed as a function of specific speed. The empirical formulae have been obtained by fitting the model test data available at that time.

According to international standard for rehabilitation and performance improvement of Hydraulic turbines [3], the internal mechanical losses may significantly lower down the efficiency of Francis turbine operating at low specific speed. Figure 1 represents a plot of loss distribution at peak efficiency depending on the specific speed N_q for a wide range of model Francis turbines in 2005. This plot gives a good idea of what one may expect in the way of performance for a totally new unit at that point of time. It can be seen that the labyrinth losses and disc friction losses contribute significantly to the turbine hydraulic losses in case when the specific speed N_q of a turbine is low.

Turbine output is decreased due to labyrinth losses (friction losses and volumetric losses - water leakage) by the nearly constant value (kW) for the whole operating range of the turbine. Their relative importance in % decreases with the flow. If labyrinth losses represent e.g. 3% at full load, they can be higher than 6% at part load.



The Tokke Model, which is under this investigation, is a high head Francis turbine with the specific speed of $N_q = 23.6$. Roughly estimated from Figure 1, the labyrinth losses and disc friction losses at this N_q are almost as high as spiral case losses, stay vane losses and guide vane losses all together. Consequently, if the internal mechanical losses are not taken into account in the CFD analysis, a higher difference between the experimental and numerical hydraulic efficiency is expected.

In previous experimental and numerical studies of the Tokke Model [4], the difference between experimental and numerical hydraulic efficiencies at best efficiency point (BEP) was rather small (0.85%), while the difference between experimental and numerical efficiencies at lower discharge turbine operation was quite significant (14%).

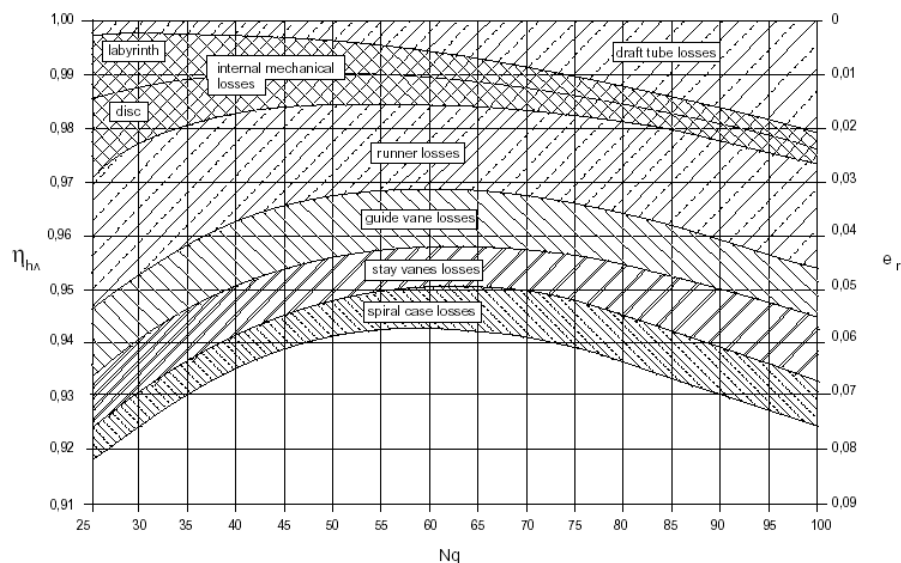


Figure 1. Efficiency and distribution of losses versus specific speed for Francis turbine [3].

This research is mainly focused on the CFD analysis of a detailed Tokke Model in order to get more accurate prediction of its hydraulic efficiency.

2. Numerical model and mesh

Numerical analyses are useful tools for making predictions about the properties of real-world problems. The accuracy of those predictions strongly depends on quality of numerical models and on simplifications adopted during the analysis in order to ensure the feasibility of a solution.

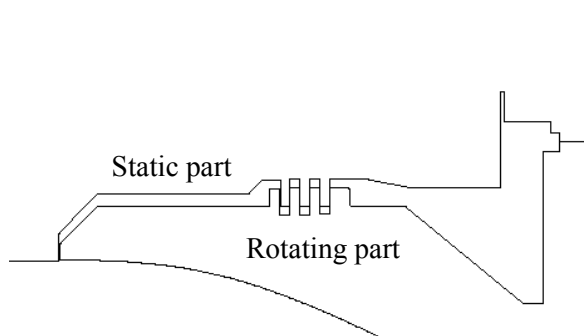


Figure 2. Runner seal on crown side.

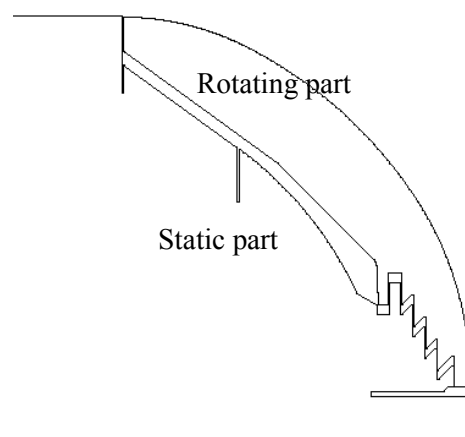


Figure 3. Runner seal on band side.

To get more accurate solution, our numerical model is built in a way to represent the conditions at test site as good as possible. The geometry of the model starts at the inlet of spiral casing and ends at the outlet of draft tube. Both runner seals as depicted in figure 2 and figure 3 are also taken into consideration. The runner seal geometry corresponds to the geometry at the test site. The only difference is that the edges inside the labyrinth are not rounded but sharp. This simplification helps to maintain the mesh size within manageable limits.



Figure 4. Computational domain.

The computational domain consists of the Spiral casing with Stay vanes, the Guide vane cascade, the Runner with labyrinths, and the Draft tube (see figure 4). The spatial discretization of the flow domain of the Spiral casing and the Draft tube was performed by IGGTM, which is an interactive geometry modeler and a grid generation system for multi-block structured grids. The spatial discretization of the flow domain of the Guide vane and the Runner with labyrinths was performed by AutoGrid5TM which is an automatic meshing system for turbo-machinery configurations.

Table 1. Grid size.

Part of the turbine	App. number of nodes
Spiral casing with a Stay vane	2.600.000
Guide vane	6.000.000
Runner	8.700.000
Labyrinths	30.100.000
Draft tube	1.000.000
Total	48.400.000

The full size 360° mesh was generated to cover potential unevenness of the flow distribution inside the turbine. Figure 5 shows the computational grid of the whole turbine, while figure 6 depicts some details about the mesh of the runner, the guide vane and the labyrinth. Information about the grid size is gathered in table 1.

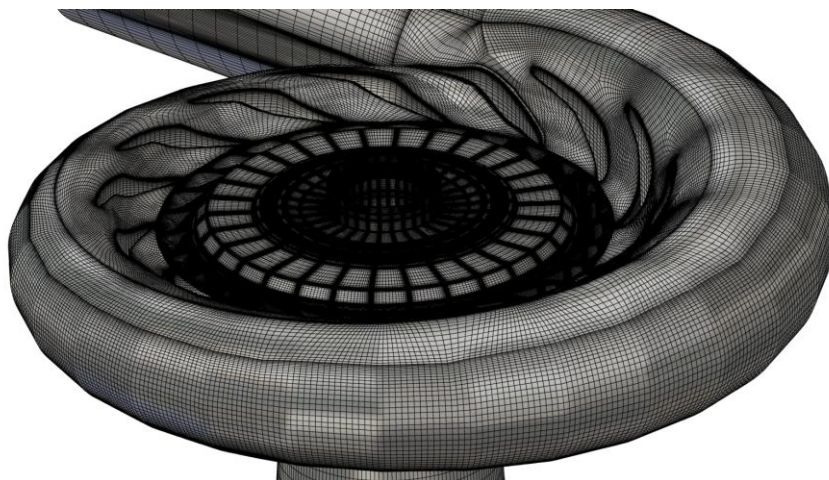


Figure 5. Computational grid.

A great care and consideration was needed while generating the mesh inside the labyrinths. The size of the mesh should be as small as possible to lower down the computational cost. However, all the significant geometrical details need to be captured with the mesh. Additionally, also the close-to-wall boundary layer has to be set correctly in order to capture the velocity gradient at the solid walls.

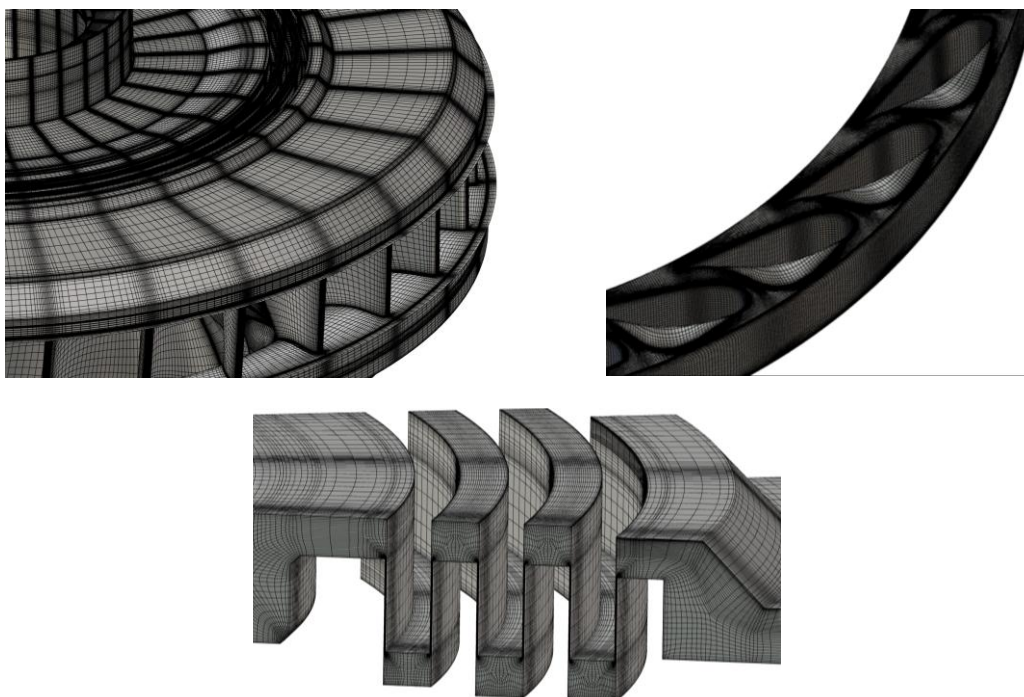


Figure 6. Computational grid in details.

3. Flow analysis

For the flow analysis the computer code Numeca FINETM/Turbo 9.02 has been used. The working fluid is water and the flow inside the turbine is assumed to be steady. The Reynolds-averaged Navier-Stokes equations for incompressible turbulent flow are adopted. The k- ω SST (Shear Stress Transport) turbulence model with extended wall function was used to provide a link between the turbulent transport of momentum and energy and mean flow properties.

A central spatial discretization scheme and a Merkle preconditioning were used. For the purpose of efficient computation and fast convergence a multigrid strategy “V-cycle” was employed [5]. Three multigrid levels with a linear progression of smoothing sweeps on successive grid levels and 100 cycles per grid level have been chosen. The amount of sweeps is the amount of times the Runge-Kutta operator is applied.

The simulation was performed for three given operating points:

- part load (PL);
- the best efficiency point (BEP);
- high load (HL).

Table 2 summarizes the operating conditions of a turbine at a test site.

Table 2. Test conditions corresponding to the operating points.

Operating point	Head (m)	Flow rate (m ³ /s)	Runner speed (Hz)	Hydraulic efficiency (%)
PL	12.29	0.07	6.77	72.5
BEP	12.77	0.21	5.74	92.4
HL	12.61	0.23	6.34	91.0

At the inlet of the computational domain the absolute total pressure was prescribed in accordance with the turbine head at the test site for a given operating point. At the outlet of the computational domain the average static pressure was prescribed.

The steady analyses were performed on a PC with an eight-core Intel i7 processor and 64GiB of RAM, running on a 64-bit Windows 7 OS. For the same computational domain including runner seals, two different Rotor/Stator approaches were taken into consideration: the frozen rotor approach (FR) and the mixing plane approach (MP).

Figure 7 and figure 8 show the y^+ at the runner and at the runner seals, respectively.

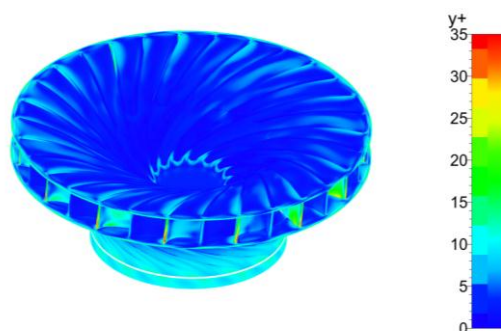


Figure 7. y^+ at the runner.

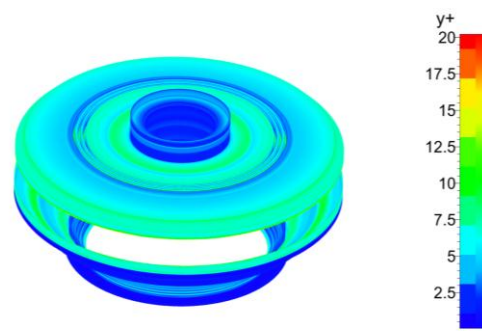


Figure 8. y^+ at the runner seals.

Our numerical model does not have balancing holes, so the flow leakage is possible only through the runner seal on a band side (see figure 3). Table 3 represents the quantities of band-seal leakage for

given three operating points. The flow through the labyrinth is almost the same for all three operation points. The leakage flow is driven only by the pressure difference, which is for all three operating points almost the same, since the head of a turbine is more or less the same.

Table 3. Mass flow through the runner seal on a band side.

	Mass flow at the Inlet of a turbine (kg/s)	Mass flow through the labyrinth (kg/s)	Proportion of the flow through the labyrinth (%)
PL	72.3	0.318	0.44
BEP	207.7	0.329	0.16
HL	237.3	0.367	0.15

As expected, the proportion of the flow lost through the labyrinth is rather small, only 0.44% at a PL operation and even smaller at BEP and HL operation. Velocity conditions inside the runner and inside the labyrinth are shown in figure 9 and in figure 10, respectively.

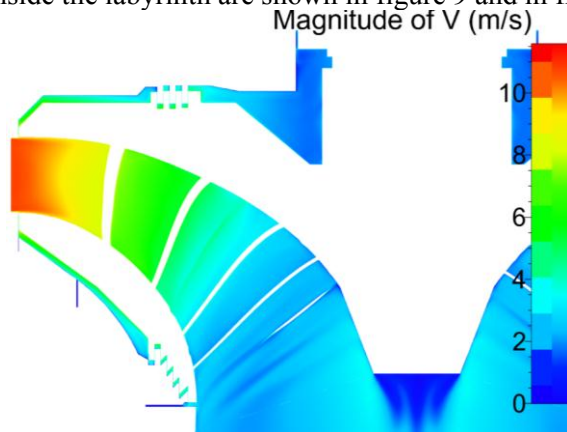


Figure 9. Velocity conditions inside the runner at a BEP operation.

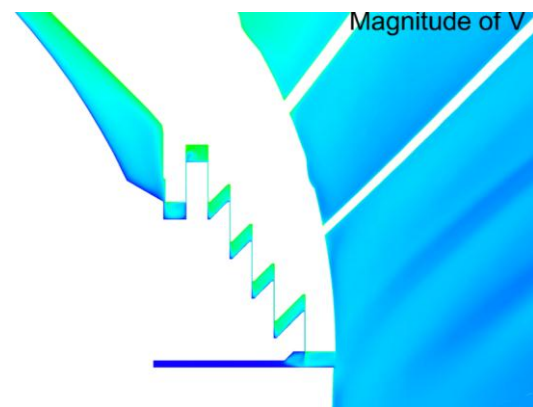


Figure 10. Velocity conditions inside the labyrinth at a BEP operation.

3.1. Pressure data validation

Time dependent pressure measurements in the stationary and rotating frames are available from the Tokke model test rig. The position of the pressure measurements are given in table 4. Our numerical analyses are stationary and, therefore, the information about the pressure fluctuations is not available. To compare our calculated pressure values to the time dependent pressure measurements, some statistical manipulation of experimental data is needed. A median pressure was calculated for the purpose of comparison with the CFD. In order to maintain the information about the pressure oscillation, the 25th percentile and the 75th percentile were calculated and shown together with the median pressure as some kind of a confidence interval.

Table 4. Position of the pressure sensors.

	VL01	DT11	DT21	P42	P71	S51
x (m)	0.2623	-0.0904	0.0904	7.16E-5	-0.0666	-0.0800
y (m)	0.1935	0.1566	-0.1566	0.1794	0.0423	0.0838
z (m)	-0.0296	-0.3058	-0.3058	-0.0529	-0.0860	-0.0509

The comparison of pressure data for each particular operation point is given in figure 11, figure 12 and figure 13, respectively. The CFD pressure data are available for both the FR approach and the MP approach.

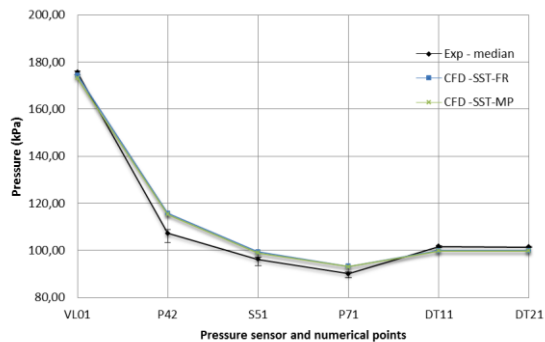


Figure 11. Comparison of experimental and numerical pressure at different locations in the turbine for PL operation.

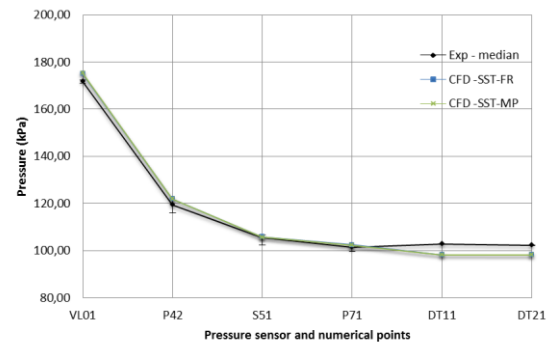


Figure 12. Comparison of experimental and numerical pressure at different locations in the turbine for BEP operation.

In the case of PL operation (see figure 11), the differences between the calculated pressure values and measured median values are the highest at the pressure side of a blade (P42, P71) and at the suction side of a blade (S51). However, at the same three positions also the pressure fluctuations were the highest. The maximal difference observed between the measured median values and numerical results was 7.8% at position P42 in the case of PL operation.

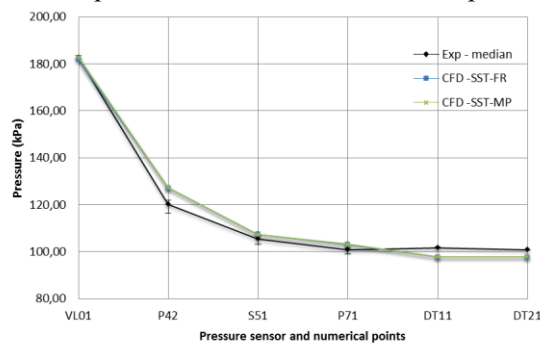


Figure 13. Comparison of experimental and numerical pressure at different locations in the turbine for HL operation.

For all three operation regimes the same trend can be observed: the pressure at points located on runner blade (P42, P71, S51) is always over-predicted, while the pressure in the draft tube (DT11, DT21) is always under-predicted. As can be seen from figure 11, figure 12 and figure 13, the pressure predictions of FR approach are in a very good agreement with the pressure predictions of MP approach.

3.2. Velocity data validation

Velocity measurements (axial and tangential) were performed with a laser Doppler anemometer (LDA) along two horizontal lines in the draft tube. The coordinates are available in table 5.

Table 5. Location of velocity measurement.

	Line 1		Line 2	
	Point 1	Point 2	Point 1	Point 2
x (m)	-0.1789	0	-0.1965	0
y (m)	0	0	0	0
z (m)	-0.2434	-0.2434	-0.5614	-0.5614

Positive axial velocity is defined in the stream-wise direction and the tangential velocity is positive in the runner rotational direction. A comparison of experimental and numerical velocities is given in figure 14 - figure 25.

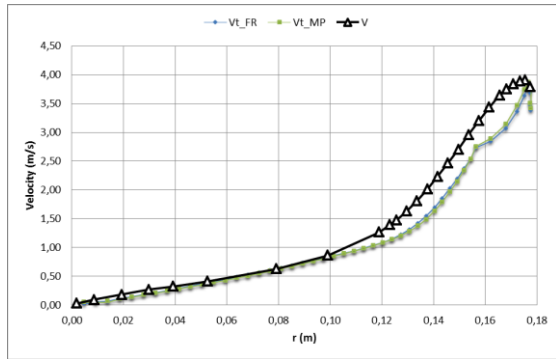


Figure 14. PL: Tangential vel. - upper line.

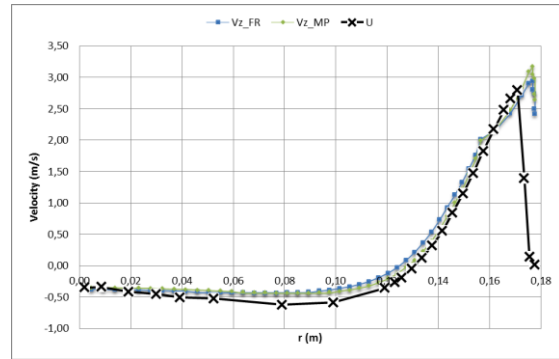


Figure 15. PL: Axial velocity – upper line.

In the case of PL operation, a very good agreement between CFD predictions and measurements is achieved, except for the tangential velocity at lower line (see figure 16). The differences between FR solution and MP solution are very small.

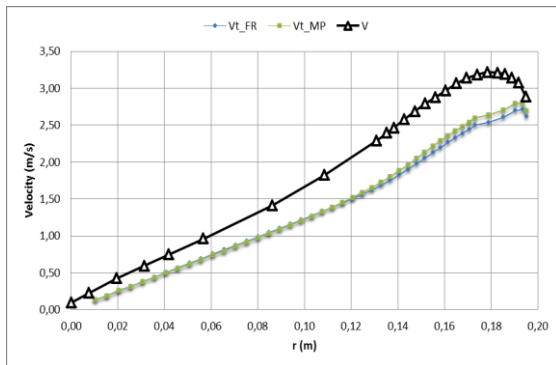


Figure 16. PL: Tangential vel. - lower line.

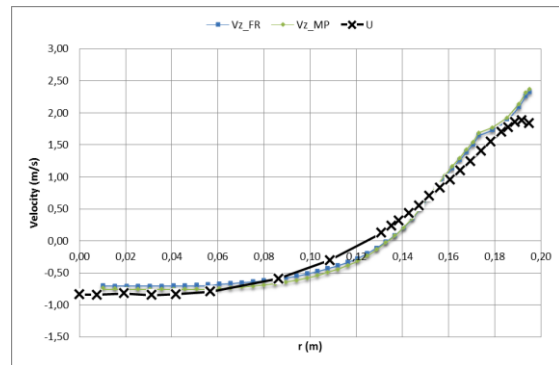


Figure 17. PL: Axial velocity – lower line.

In case of BEP operation, there is a noticeable difference between FR and MP solution. The latter generally better predicts the shape of both tangential velocity profile and axial velocity profile. The predictions of tangential velocity are better in the close-wall region ($r > 0.1\text{m}$) and worse in the center region ($r < 0.1\text{m}$).

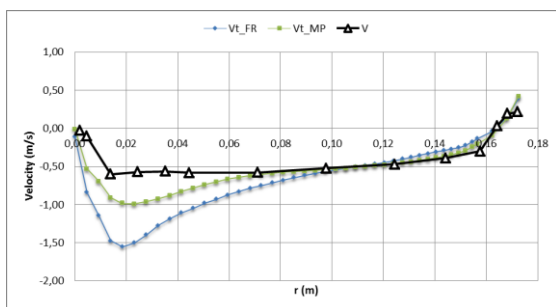


Figure 18. BEP: Tangential vel. - upper line.

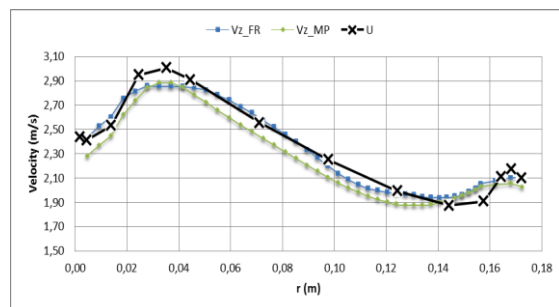


Figure 19. BEP: Axial velocity – upper line.

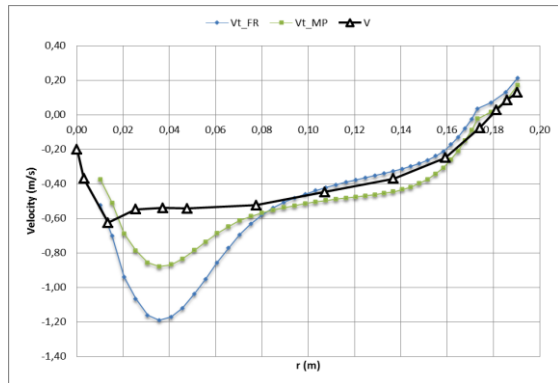


Figure 20. BEP: Tangential vel. - lower line.

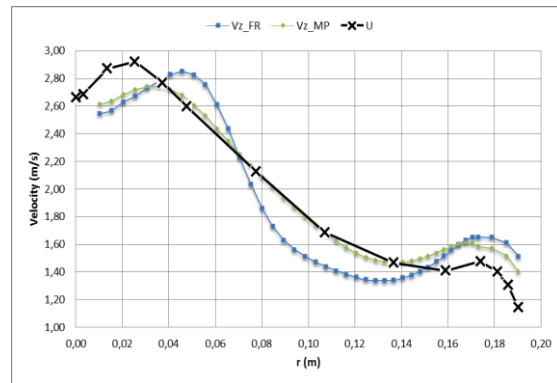


Figure 21. BEP: Axial velocity – lower line.

In a HL operation case, the predictions of tangential velocity are not as good as they were in case of BEP operation. In general, the predictions at upper line are for all three operation cases better than the predictions at lower line. Higher discrepancies between measured and calculated velocities could be the consequence of a fact that the SST turbulence model in Numeca FINETM/Turbo 9.02 does not include curvature correction.

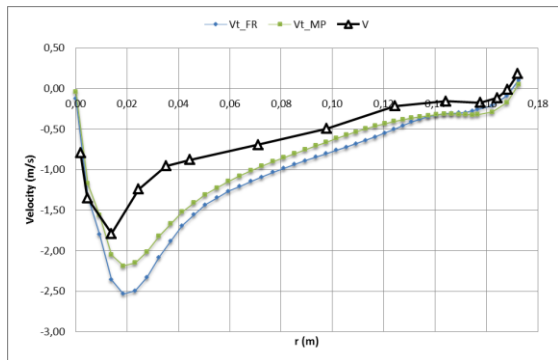


Figure 22. HL: Tangential vel. - upper line.

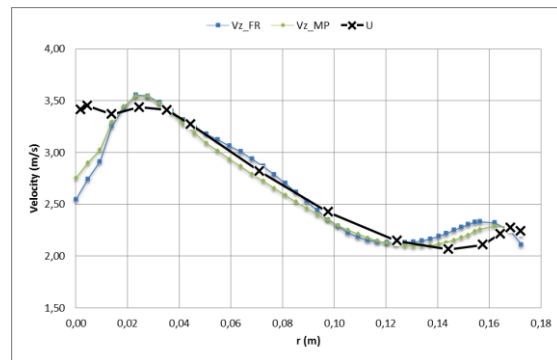


Figure 23. HL: Axial velocity – upper line.

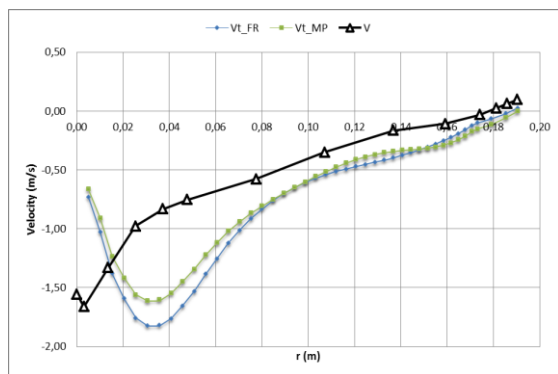


Figure 24. HL: Tangential vel. - lower line.

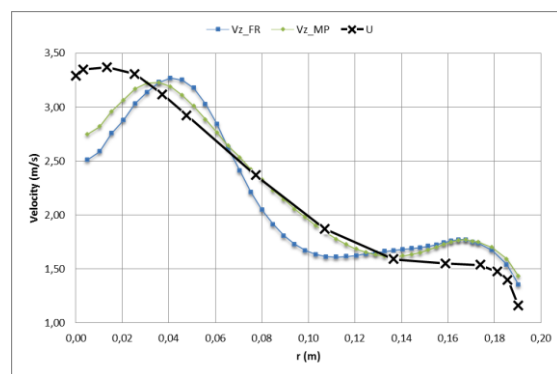


Figure 25. HL: Axial velocity – lower line.

3.3. Efficiency and torque

As a final result of CFD simulations, for each of the three given operating points the hydraulic efficiency of the turbine was calculated. The comparison of measured and predicted efficiencies is

given in figure 26. The notation “NoLab” represent the solution, which is identical to FR solution, except that no runner seals are taken into account.

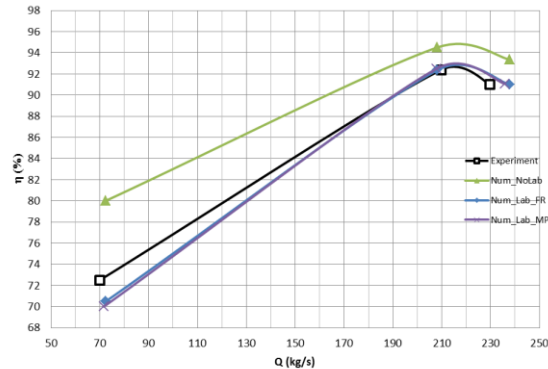


Figure 26. Hydraulic efficiency of a turbine at given operating points.

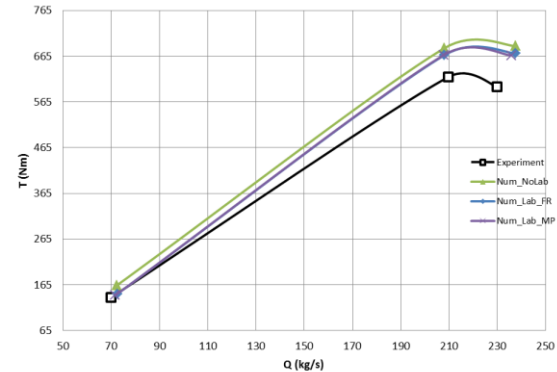


Figure 27. Torque of a turbine at given operating points.

From figure 26 it is evident that with the consideration of labyrinths much better prediction of hydraulic efficiency is achieved. By including the labyrinths to the numerical solution, the maximum difference between the experimental and numerical efficiencies at PL turbine operation lowers down from 7% to 2%. The efficiency predictions at BEP and HL operation points are in that case within 0.1% consistent with measurements. It is rather interesting that the efficiency predictions at PL operation are even under-predicted.

The comparison of measured and calculated torque is shown in figure 27. The best match between measured and predicted torque is achieved at PL operation. At BEP and HL operation the torque is over-estimated. There is a very good agreement between FR and MP solution. The torque curve of a “NoLab” solution is parallel to FR and MP solution curves. That indicates the influence of runner seals on the turbine torque.

4. Conclusion

In present study, a CFD investigation of a high head model Francis turbine was carried out. All geometrical details of a Tokke turbine, including runner seals, were taken into consideration. Steady state numerical simulations were performed at three representative operating points and validated with available experimental data. Except for a small change in the shape of velocity profile curves, there is no noticeable difference between FR and MP solution. A very good agreement between measured and predicted pressure values was achieved. The maximum difference occurred at the same point where the pressure fluctuations in a measured time dependent signal were the highest. Also the validated tangential and axial velocities in the draft tube were not far from measured values. However, the predictions of the velocities at upper line position were better than those located at lower line.

Including the runner seals, a very good prediction of the hydraulic efficiency compared to the experimental data was achieved. Instead of 7% over-prediction at PL operation, a 2% under-prediction was obtained. The influence of runner seals on the turbine torque was rather small. Also the proportion of the flow which leaked through the labyrinth was small, with the maximum amount of 0.44% at PL operation. Therefore, the main reason for the efficiency drop was in the labyrinth losses and disc friction losses. Especially at part load operation those losses significantly lowered down the turbine hydraulic efficiency. The influence of labyrinth losses on the turbine hydraulic efficiency decreased with the increase of the flow through the turbine.

Acknowledgements

The authors gratefully acknowledge the sponsorship of Scandic Energy.

References

- [1] Zhao W, Nielsen T K and Billdal J T, 2010 Effects of cavity on leakage loss in straight-through labyrinth seals *IOP Conf. Series: Earth and Environmental Science* **12**
- [2] Kurokawa J and Kitahora T, 1994 Accurate determination of volumetric and mechanical efficiencies and leakage behaviour of Francis turbine and Francis pump-turbine *Proc. XVII IAHR (Beijing)*
- [3] IEC 62256:2008 83-84
- [4] Chirag T, Cervantes M J, Gandhi B K and Dahlhaug O G, 2013 Experimental and numerical studies for a high head Francis turbine at several operating points *Journal of Fluid Engineering* **135**
- [5] FINETM/Turbo v9.0, 2013 Discretization and Solution Theory *Theoretical manual* 5-11